Unifying geometric entanglement and geometric phase in a quantum phase transition

Vahid Azimi Mousolou,[1,*] Carlo M. Canali,[1,†] and Erik Sjöqvist[2,3,‡]

[1]*Department of Physics and Electrical Engineering, Linnaeus University, 391 82 Kalmar, Sweden*

[2]*Department of Quantum Chemistry, Uppsala University, Box 518, Se-751 20 Uppsala, Sweden*

[3]*Centre for Quantum Technologies, National University of Singapore, 3 Science Drive 2, 117543 Singapore, Singapore*

Geometric measure of entanglement and geometric phase have recently been used to analyze quantum phase transition in the XY spin chain. We unify these two approaches by showing that the geometric entanglement and the geometric phase are respectively the real and imaginary parts of a complex-valued geometric entanglement, which can be investigated in typical quantum interferometry experiments. We argue that the singular behavior of the complex-value geometric entanglement at a quantum critical point is a characteristic of any quantum phase transition, by showing that the underlying mechanism is the occurrence of level crossings associated with the underlying Hamiltonian.

Quantum phase transitions (QPTs) are qualitative changes in the properties of many-body systems driven by quantum fluctuations at zero temperature. A key feature to understand the nature of QPTs is the quantum correlations between the system degrees of freedom, which at the critical point bring about an intersection of the ground-state and excited-state energy levels. While QPTs have traditionally been characterized by appropriate correlation functions [1,2], many researchers have recently addressed this problem from a quantum information perspective. One idea along this line is to use measures of entanglement to characterize QPTs. Indeed, there has been a great deal of work analyzing properties of quantum entanglement in many-body systems undergoing QPT [3–5]. Another idea is based on the fact that nontrivial geometric phases (GPs) are strongly affected by quantum and classical correlations residing in the many-body quantum states [6], and especially by the level degeneracies associated with QPTs in such systems. Therefore GPs can also be used to detect the presence of a QPT. Relations between GP and QPTs have been established theoretically [7–9] and experimentally in NMR [10].

In this paper, we examine the geometric measure of entanglement (GE) [4,11,12] and GPs in the vicinity of QPT in an XY spin chain. We determine the relation between these geometric objects, allowing us to identify them as the real and imaginary part of a single measurable quantity, which we call the complex-valued GE. We demonstrate that the complex GE is accessible in interferometry experiments. The established relation is valid for a general quantum many-body system. At a quantum critical point both real and imaginary parts of the complex-valued GE display the same singular behavior, which in turn is closely associated with the singular behavior of the quantum geometric tensor triggered by a level degeneracy. This provides a universal approach to the study of quantum critical phenomena.

Consider the one-dimensional XY model system with N sites in a transverse magnetic field. The corresponding

Hamiltonian reads

$$H(r,h) = -\sum_{j=1}^{N} \left(\frac{1+r}{2}\sigma_j^x \sigma_{j+1}^x + \frac{1-r}{2}\sigma_j^y \sigma_{j+1}^y + h\sigma_j^z \right), \tag{1}$$

with a periodic boundary condition such that the first and $(N+1)$th sites are identified. Here, r is the anisotropy parameter, h is the magnetic field strength, and σ_j^k, $k = x,y,z$, are the standard Pauli operators of the jth spin. In the thermodynamic limit ($N \to \infty$), the system described by Eq. (1) undergoes a QPT at $h = h_c = 1$. The full phase diagram can be found in Refs. [2,13]. In the anisotropy range $0 < r \leqslant 1$ the system belongs to the Ising universality class. The isotropic case $r = 0$ corresponds to the XX model, which belongs to the Berezinsky-Kosterlitz-Thouless universality class. The standard procedure to solve the eigenvalue problem of $H(r,h)$ is to convert the spin operators into fermionic operators, using successively Jordan-Wigner, Fourier, and Bogoliubov transformations [14]. The ground state in the even-fermion-number sector can be expressed in terms of fermionic modes c_j as

$$|\psi(r,h)\rangle$$
$$= \prod_{m=0}^{m<\frac{N-1}{2}} [\cos\theta_m(r,h) + i\sin\theta_m(r,h)c_m^\dagger c_{N-m-1}^\dagger]|\uparrow...\uparrow\rangle, \tag{2}$$

with $\tan 2\theta_m(r,h) = r\sin\frac{\pi(2m+1)}{N}/(h - \cos\frac{\pi(2m+1)}{N})$ [4]. For $0 < r \leqslant 1$ the ground state in the thermodynamic limit is doubly degenerate in the ferromagnetic regime $h < 1$ and singly degenerate for $h > 1$, with the critical value for $h_c = 1$ being a point of conical intersection.

Entanglement of the ground state $|\psi(r,h)\rangle$ can be measured by approximating it by the closest pure product state [12]. This state is given by the maximal overlap

$$\Lambda_{\max}(r,h) = \max_{\Phi} |\langle\Phi|\psi(r,h)\rangle|, \tag{3}$$

over all pure product states Φ. The resulting number $\Lambda_{\max}(r,h)$ is the entanglement eigenvalue of the XY ground state [12]. GE of the ground state is quantified via [4]

$$E_{\log_2}[\psi(r,h)] = -\log_2 \Lambda_{\max}^2(r,h), \tag{4}$$

*vahid.mousolou@lnu.se

†carlo.canali@lnu.se

‡erik.sjoqvist@kvac.uu.se

which in the thermodynamic limit is characterized by the geometric entanglement density

$$\varepsilon(r,h) = \lim_{N \to \infty} \varepsilon_N(r,h), \tag{5}$$

where $\varepsilon_N(r,h) = E_{\log_2}[\psi(r,h)]/N$ is the entanglement per site. Using the translational symmetry of $|\psi(r,h)\rangle$, the closest pure product state for each value of r and h takes the form [4]

$$|\Phi(\xi)\rangle = \otimes_{j=1}^{N}\left[\cos\left(\frac{\xi}{2}\right)|\uparrow\rangle_j + \sin\left(\frac{\xi}{2}\right)|\downarrow\rangle_j\right], \tag{6}$$

where the parameter ξ is chosen so as to maximize the overlap, i.e., $\Lambda_{\max}(r,h) = \max_\xi |\langle\Phi(\xi)|\psi(r,h)\rangle| \equiv |\langle\Phi(\xi_{\max})|\psi(r,h)\rangle|$. By using Eq. (5), one obtains the GE density [4]

$$\varepsilon(r,h) = -\frac{2}{\ln 2}\max_\xi \int_0^{1/2} d\mu \ln[\cos\theta(\mu,r,h)\cos^2(\xi/2)$$
$$+ \sin\theta(\mu,r,h)\sin^2(\xi/2)\cot\pi\mu], \tag{7}$$

with $\tan 2\theta(\mu,r,h) = r\sin 2\pi\mu/(h - \cos 2\pi\mu)$.

It has been shown [4] that features of quantum criticality, such as universality, critical exponents, and scaling, are captured by the singular behavior of the GE of the XY ground state. The critical exponents for different universality classes have been found by scaling analysis of divergences at the singular points of the GE density. The singular behavior of the GE density at the critical point $h_c = 1$ is shown in Fig. 1, where $\partial\varepsilon_N(r,h)/\partial h$ has been plotted as function of magnetic field h for different values of r in the thermodynamic limit. In the inset we plot the same quantity for an Ising model for finite values of N. The cusp at $h_s > 1$ for $0 < r \leqslant 1$, coalescing with the singularity at $h_c = 1$ as $r \to 0$, is an interesting feature related to properties of the closest product state $\Phi(\xi_{\max})$. For each $0 \leqslant r \leqslant 1$ there is a finite value of $h = h_s$ for which $\xi_{\max}$ vanishes and $\Phi(\xi_{\max})$ is polarized in the z direction [4]. This state remains the closest pure product state for all $h > h_s$, causing a discontinuity jump in the second derivative of $\varepsilon(r,h)$ at $h = h_s$.

Recently, a generic connection between GPs and QPTs has been identified [7]. A scaling analysis of GP of the XY ground state reveals similar information about quantum criticality as the GE density. The top panel in Fig. 2 shows the behavior of the GP per site $\beta_N^g(r,h)$ of the XY ground state, accumulated
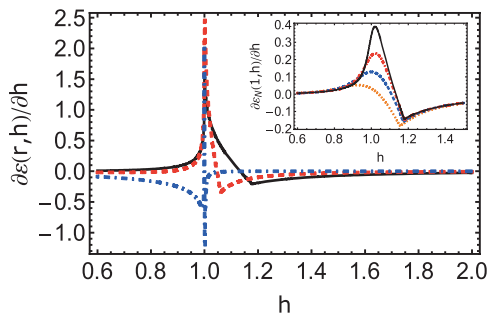

FIG. 1. (Color online) Derivative of the ground-state GE density $\varepsilon(r,h)$ of the XY model as a function of the magnetic field h in the thermodynamic limit. Solid curve: Ising limit ($r = 1$); dashed curve: anisotropic ($r = 0.5$) XY model; and dot-dashed curve: anisotropic ($r = 0.05$) XY model. The inset corresponds to the Ising limit for different lattice sizes $N = 11, 18, 31, 64$.
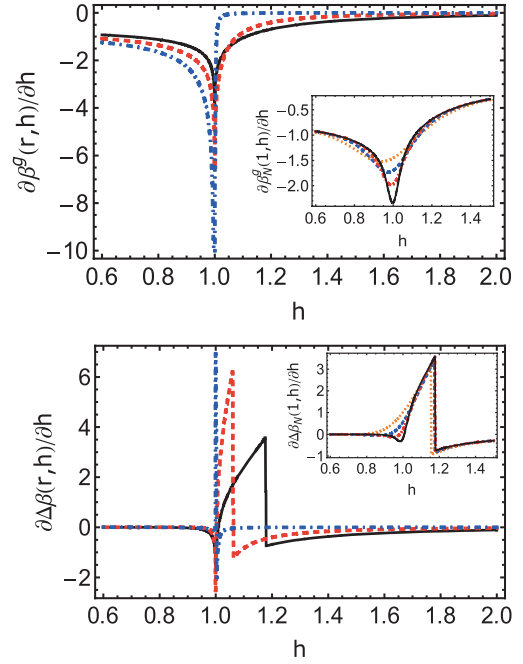

FIG. 2. (Color online) Top panel: Derivative of the GP density, GP per particle, corresponding to cyclic evolution of the XY ground state given in Eq. (8), as a function of the magnetic field h in the thermodynamic limit. Lower panel: h derivative of the difference between GP densities corresponding to the evolutions given in Eqs. (8) and (9), plotted as a function of magnetic field h in the thermodynamic limit. Solid curve: Ising limit ($r = 1$); dashed curve: anisotropic ($r = 0.5$) XY model; dot-dashed: anisotropic ($r = 0.05$) XY model. The insets correspond to the Ising limits for different finite lattice sizes $N = 11, 18, 31, 64$.

by adiabatically rotating each spin around the z axis via

$$C_g^{(r,h)} : [0,\pi] \ni \phi \to U_{\text{tot}}(\phi)|\psi(r,h)\rangle\langle\psi(r,h)|U_{\text{tot}}^\dagger(\phi), \tag{8}$$

where $U_{\text{tot}}(\phi) = \otimes_{j=1}^N U_j(\phi) = \otimes_{j=1}^N \exp(\frac{i\sigma_j^z\phi}{2})$, for different lattice size N. $\beta^g(r,h) = \lim_{N\to\infty}\beta_N^g(r,h)$ is the GP density, i.e., the GP per site in the thermodynamic limit.

The lower panel of Fig. 2 displays the behavior of the difference between the GPs per site associated with $C_g^{(r,h)}$ and the evolution

$$C_p^{(r,h)} : [0,\pi] \ni \phi \to U_{\text{tot}}(\phi)|\Phi(r,h)\rangle\langle\Phi(r,h)|U_{\text{tot}}^\dagger(\phi) \tag{9}$$

of the closest pure product state $|\Phi(r,h)\rangle \equiv |\Phi(\xi_{\max})\rangle$. $C_p^{(r,h)}$ is a path of pure product states along which each instant state is the closest pure product state of the corresponding instant ground state along the path $C_g^{(r,h)}$. The entanglement is fixed along this pair of paths. The associated GP difference is in this sense related to the entanglement residing in the initial ground state $|\psi(r,h)\rangle$.

In the thermodynamic limit, we obtain the GP densities

$$\beta^g(r,h) = \lim_{N\to\infty}\beta_N^g(r,h) = 2\pi\int_0^{1/2}\sin^2\theta(\mu,r,h)d\mu,$$
$$\beta^p(r,h) = \lim_{N\to\infty}\beta_N^p(r,h) = 2\pi\sin^2(\xi_{\max}/2), \tag{10}$$

corresponding to $C_g^{(r,h)}$ and $C_p^{(r,h)}$, respectively.

The GP density difference is

$$\Delta\beta(r,h) \equiv \beta^g(r,h) - \beta^p(r,h). \qquad (11)$$

For $0 < r \leqslant 1$, $\Delta\beta(r,h)$ displays the same (Ising universality class) critical behavior at $h = h_c$ as $\varepsilon(r,h)$. Interestingly, even the cusp in $\varepsilon(r,h)$ at $h_s > h_c$ is captured by $\Delta\beta(r,h)$ [now in the form of a discontinuous jump in the first derivative of $\Delta\beta(r,h)$], while the ground-state GP density $\beta^g(r,h)$ is smooth on this h interval.

For the XX model ($r = 0$), we observe that $\Delta\beta(0,h) = 0$ and therefore $\frac{\partial}{\partial h}\Delta\beta(0,h) = 0$ for the specific evolution operator $U_{\text{tot}}(\phi)$ [15]. On the other hand, as indicated in the lower panel of Fig. 2, $\frac{\partial}{\partial h}\Delta\beta(r,h)$ is singular at $h = h_c = 1$ when $r \neq 0$. Thus,

$$\lim_{r \to 0} \frac{\partial\Delta\beta(r,h)}{\partial h}\bigg|_{h=h_c} \neq \frac{d\Delta\beta(0,h)}{dh}\bigg|_{h=h_c}, \qquad (12)$$

which shows that the XX criticality is detected by a nonsmooth contractible phase difference. Arguments along this line have been used in Refs. [8,16] to locate the criticality of XX model by using GP. From the analysis of Ref. [4], we see that also $\partial\varepsilon(r,h)/\partial r$ scales differently for $r \neq 0$ and $r = 0$ near the critical point. Just as in the case of GE density, the nature of Eq. (12) identifies the different universality classes of the XY spin chain.

We now give a unifying operational interpretation of GP and GE for the XY system, in the context of interferometry. Let $|0\rangle,|1\rangle$ span the state space of an auxiliary qubit, playing the role of the two interferometer arms. Prepare the initial state $|\Psi_i\rangle = \frac{1}{\sqrt{2}}(|0\rangle + |1\rangle)|\psi(r,h)\rangle$. In the $|1\rangle$ arm, project onto the product state $|\Phi(\xi)\rangle$ given in Eq. (6). The two spin chain states $|\psi(r,h)\rangle$ and $|\Phi(\xi)\rangle$ are exposed to the parallel transporting unitary operators $U_\psi^\parallel(\phi) = \otimes_{j=1}^N e^{\frac{i}{2}\phi(\sigma_j^z - \langle\psi(r,h)|\sigma_j^z|\psi(r,h)\rangle)}$ and $U_\Phi^\parallel(\phi) = \otimes_{j=1}^N e^{\frac{i}{2}\phi(\sigma_j^z - \langle\Phi(\xi)|\sigma_j^z|\Phi(\xi)\rangle)}$, respectively, where $\phi \in [0,\pi]$. Note that $U_\psi^\parallel(\phi)$ and $U_\Phi^\parallel(\phi)$ are the same unitary up to an overall phase factor, which assures that $|\langle\Phi(\xi)|U_\Phi^{\parallel\dagger}U_\psi^\parallel|\Psi(r,h)\rangle|$ for given r and h is a function of ξ only. The resulting state $U_\Phi^\parallel(\pi)|\Phi(\xi)\rangle$ in the $|1\rangle$ arm is parallel transported along the shortest geodesic back to $|\Phi(\xi)\rangle$, while a U(1) shift e^{-if} is applied to the $|0\rangle$ arm. Finally, the two arms are brought back to interfere, resulting in the final state,

$$|\Psi_f\rangle = \tfrac{1}{2}|0\rangle\big[e^{i(\varphi^g - f)}|\psi(r,h)\rangle + e^{i\varphi^p}|\Phi(\xi)\rangle\langle\Phi(\xi)|\psi(r,h)\rangle\big] + \cdots, \qquad (13)$$

with φ^g and φ^p being the GPs associated with the evolution of $|\psi(r,h)\rangle$ and $|\Phi(\xi)\rangle$, respectively. The intensity in the $|0\rangle$ arm becomes

$$\mathcal{I}_0 = \tfrac{1}{4}[1 + |\langle\Phi(\xi)|\psi(r,h)\rangle|^2] + \tfrac{1}{2}\text{Re}[A(r,h;\xi)e^{-if}], \qquad (14)$$

where

$$A(r,h;\xi) = \langle\psi(r,h)|e^{-i\varphi^p}|\Phi(\xi)\rangle\langle\Phi(\xi)|e^{i\varphi^g}|\psi(r,h)\rangle$$
$$= |\langle\Phi(\xi)|\psi(r,h)\rangle|^2 e^{i\Delta\varphi}. \qquad (15)$$

Here, $|A(r,h;\xi)| = |\langle\Phi(\xi)|\psi(r,h)\rangle|^2$ and $\arg A(r,h;\xi) = \Delta\varphi$ characterize the visibility and phase shift of the interference fringes obtained by varying f. Note that $A(r,h;\xi)$ is unchanged under any local gauge transformation and reparametrization of the paths. The entanglement eigenvalue

$\Lambda_{\max}(r,h)$ and the GP difference $\Delta\varphi(r,h)$ associated with $C_g^{(r,h)}$ and $C_p^{(r,h)}$ can be read-out from the interference fringes by tuning the single parameter ξ to the value $\xi_{\max}$ giving the maximal visibility.

Following the procedure leading to GE, we introduce a complex-valued GE, being defined as the following extensive entanglement sensitive quantity:

$$E_{\log_2}^c[\psi(r,h)] = -\log_2 A(r,h;\xi_{\max})$$
$$= E_{\log_2}[\psi(r,h)] - i\frac{\Delta\varphi(r,h)}{\ln 2}. \qquad (16)$$

The properties of the quantum critical point are characterized by both the real and imaginary parts of the complex-valued GE density:

$$\varepsilon_c(r,h) = \lim_{N \to \infty} \frac{1}{N} E_{\log_2}^c[\psi(r,h)] = \varepsilon(r,h) - i\frac{\Delta\beta(r,h)}{\ln 2}. \qquad (17)$$

The GE and GP densities are thus two different sides of the same coin: the complex-valued GE density $\varepsilon_c(r,h)$.

Let us now generalize the above ideas to a generic N-body system. Assume that the system is prepared in the state $|\Psi\rangle$ and thereafter evolves around a loop C_Ψ generated by a one-parameter family of local unitary operators $U(t) = \otimes_j^N U_j(t)$, with $U_j(t)$ acting on subsystem j. The closest product state $|\Phi\rangle$ evolves under the same $U(t)$. Note that the resulting C_Φ is in general an open path. Let $\Delta\varphi(\Psi) = \varphi(\Psi) - \varphi(\Phi)$ be the GP difference associated with paths C_Ψ and C_Φ. By following the above interferometer scheme, the interference fringes are characterized by

$$A(\Psi) = \Lambda_{\max}^2(\Psi)e^{i\Delta\varphi(\Psi)}, \qquad (18)$$

with $|\Phi\rangle$ chosen to maximize the visibility. Similar to the XY case discussed above, $A(\Psi)$ can be used to define complex-valued GE of the N-body system prepared in Ψ. Furthermore, $A(\Psi)$ can be interpreted in terms of the Hermitian metric $\mathcal{T}$ on the projective state manifold $\mathcal{P}(\mathcal{H})$ [17]. This metric tensor is defined as $\mathcal{T}(v,u) = \langle v|(1 - |\psi\rangle\langle\psi|)|u\rangle$ for tangent vectors u and v at a state $|\psi\rangle\langle\psi| \in \mathcal{P}(\mathcal{H})$. We can write $\mathcal{T} = \mathcal{G} - i\mathcal{F}$, where $\mathcal{G}$ is the Riemannian metric providing the Fubini-Study measure of distance in $\mathcal{P}(\mathcal{H})$ and $\mathcal{F}$ is the symplectic curvature 2-form responsible for the GP. Let $ds^2 = \mathcal{G}(v,v)$ for each tangent vector v to $\mathcal{P}(\mathcal{H})$ denote the square of the line element associated with metric $\mathcal{G}$. Then, we have

$$\Lambda_{\max}(\Psi) = 1 - \frac{1}{2}\left[\int_G ds\right]^2, \quad \Delta\varphi(\Psi) = \int_S \mathcal{F}, \quad (19)$$

where G is a geodesic in state space connecting Ψ and Φ, and S is the oriented surface with boundary $\partial S = C_\Psi * G * G_\Phi^{-1} * C_\Phi^{-1} * G^{-1}$. The inverse denotes the reverse direction along the corresponding path (see Fig. 3). Equation (19) provides a physical realization of the Hermitian metric $\mathcal{T}$ in terms of the complex-valued GE, which is accessible in an interferometer.

A general relation between QPTs and the geometrical objects ds and $\mathcal{F}$ have been pointed out in Refs. [7,18], where the external parameter $\lambda \in \mathcal{M}$ was incorporated into the system. This relation can be understood basically by pulling back the Hermitian metric $\mathcal{T}$ on $\mathcal{M}$ via the map $\Psi_0 : \mathcal{M} \ni \lambda \longrightarrow |\psi_0(\lambda)\rangle\langle\psi_0(\lambda)| \in \mathcal{P}(\mathcal{H})$, where $|\psi_0(\lambda)\rangle$ is the unique ground state of the corresponding Hamiltonian
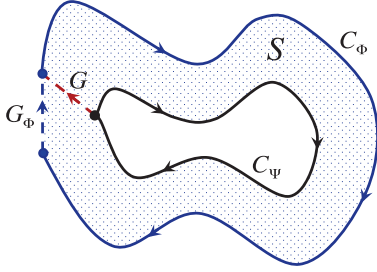
FIG. 3. (Color online) Paths C_Ψ and C_Φ of many-body state Ψ and its closest product state Φ, respectively. G is a geodesic in state space projecting Ψ onto Φ.

$H(\lambda)$. For a coordinate system on $\mathcal{M}$, the components of the pull-back tensor $T = \Psi_0^* \mathcal{T}$ are

$$T_{\mu\nu} = \sum_{n \neq 0} \frac{\langle \psi_0(\lambda)|\partial_\mu H|\psi_n(\lambda)\rangle\langle\psi_n(\lambda)|\partial_\nu H|\psi_0(\lambda)\rangle}{[E_0(\lambda) - E_n(\lambda)]^2}, \quad (20)$$

where $\psi_n(\lambda)$ are eigenstates of the system and the indices $\mu,\nu = 1,\ldots,\dim\mathcal{M}$ are labeling the coordinates of $\mathcal{M}$. The tensor T is known as quantum geometric tensor, whose imaginary part is the Berry curvature on $\mathcal{M}$ [19] and the real part provides an approximation of the fidelity of two ground states associated to neighboring points on $\mathcal{M}$ [18]. Unlike the physical interpretation of T, the above interpretation of $\mathcal{T}$ as complex-valued GE is exact and does not depend on any approximation.

The energy denominators $E_n(\lambda) - E_0(\lambda)$ in Eq. (20) show that in the thermodynamic limit, ReT and ImT will show a singular behavior at the QPT, as a QPT occurs at level crossing or avoided level crossing. This singularity is then reflected in

$\Lambda_{\max}[\psi_0(\lambda)]$ and $\Delta\varphi[\psi_0(\lambda)]$ through the expressions given in Eq. (19). Therefore it can be captured by both GE and GP difference, which are respectively the real and imaginary parts of the complex-valued GE. This source of singularity has been brought up in the Berry phase and fidelity approaches [7,18]. Our analysis suggests that the critical behavior at QPT in the GE and thus in the complex-valued GE of a generic many-body ground state comes from the same source.

In summary, we have established a unifying connection between the GP and the GE in a generic many-body system. They are respectively the real and imaginary part of a generalized complex-valued GE and they both become singular at a QPT. We have given an exact geometrical interpretation of the complex-valued GE in terms of the induced Hermitian metric on the projective Hilbert state space. Finally, we have proposed one common source for the critical behavior of the GE at any QPT. The approach presented here can be tested experimentally in an interferometry setup, where the geometric entanglement would then yield the visibility of the interference fringes, whereas the geometric phase would describe the phase shifts. The resulting interference fringes would therefore display large fluctuations at the critical point. A test-bed experiment to demonstrate the relevance of the complex-valued geometric entanglement in translational symmetric few-qubit ground states would be within reach in, e.g., NMR systems.

[1] S. Sachdev, *Quantum Phase Transitions* (Cambridge University Press, Cambridge, UK, 1999).

[2] M. Henkel, *Conformal Invariance and Critical Phenomena* (Springer, Berlin, 1999).

[3] A. Osterloh, L. Amico, G. Falci, and R. Fazio, Nature (London) **416**, 608 (2002); T. J. Osborne and M. A. Nielsen, Phys. Rev. A **66**, 032110 (2002).

[4] T.-C. Wei, D. Das, S. Mukhopadyay, S. Vishveshwara, and P. M. Goldbart, Phys. Rev. A **71**, 060305(R) (2005); T.-C. Wei, S. Vishveshwara, and P. M. Goldbart, Quantum Inf. Comput. **11**, 326 (2011).

[5] R. Orús, Phys. Rev. Lett. **100**, 130502 (2008); R. Orús, S. Dusuel, and J. Vidal, *ibid.* **101**, 025701 (2008); R. Orús and H.-H. Tu, Phys. Rev. B **83**, 201101(R) (2011); R. Orús, T.-C. Wei, and H.-H. Tu, *ibid.* **84**, 064409 (2011); W. Son, L. Amico, R. Fazio, A. Hamma, S. Pascazio, and V. Vedral, Europhys. Lett. **95**, 50001 (2011).

[6] M. S. Williamson and V. Vedral, Phys. Rev. A **76**, 032115 (2007).

[7] S. L. Zhu, Phys. Rev. Lett. **96**, 077206 (2006).

[8] A. C. M. Carollo and J. K. Pachos, Phys. Rev. Lett. **95**, 157203 (2005).

[9] G. Chen, J. Li, and J.-Q. Liang, Phys. Rev. A **74**, 054101 (2006); H. T. Cui, K. Li, and X. X. Yi, Phys. Lett. A **360**, 243 (2006); L.-C. Wang, J.-Y. Yan, and X. X. Yi, Chin. Phys. B **19**, 040512 (2010); J. Lian, J.-Q. Liang, and G. Chen, Europhys. J. B **85**, 207 (2012).

[10] X. Peng, S. Wu, J. Li, D. Suter, and J. Du, Phys. Rev. Lett. **105**, 240405 (2010); F. M. Cucchietti, J.-F. Zhang, F. C. Lombardo, and P. I. Villar, and R. Laflamme, *ibid.* **105**, 240406 (2010).

[11] A. Shimony, Ann. NY Acad. Sci. **755**, 675 (1995); D. C. Brody and L. P. Hughston, J. Geom. Phys. **38**, 19 (2001).

[12] T.-C. Wei and P. M. Goldbart, Phys. Rev. A **68**, 042307 (2003).

[13] E. Barouch and B. M. McCoy, Phys. Rev. A **3**, 786 (1971).

[14] E. Lieb, T. Schultz, and D. Mattis, Ann. Phys. (NY) **16**, 407 (1961); E. Barouch and B. M. McCoy, Phys. Rev. A **2**, 1075 (1970); S. Katsura, Phys. Rev. **127**, 1508 (1962).

[15] Note that the GE density $\varepsilon(0,h)$ vanishes above the critical point $h > h_c = 1$, while it is positive below h_c [4]. So, $|\psi(0,h)\rangle$ and $|\Phi(0,h)\rangle$ coincide only above h_c; below h_c these two states differ and may therefore pick up different GPs under general local unitary evolutions that differ from $U_{\text{tot}}(\phi)$. Therefore

$|\Delta\beta(0, h < h_c)| \geqslant 0$, while $\Delta\beta(0, h > h_c) = 0$ for a general local unitary evolution.

[16] A. Hamma, arXiv:quant-ph/0602091.

[17] J. P. Provost and G. Vallee, Commun. Math. Phys. **76**, 289 (1980).

[18] L. Campos Venuti and P. Zanardi, Phys. Rev. Lett. **99**, 095701 (2007); P. Zanardi, P. Giorda, and M. Cozzini, *ibid.* **99**, 100603 (2007).

[19] M. V. Berry, Proc. R. Soc. A **329**, 45 (1984).